First MINOS Results from the NuMI Beam

Nathaniel Tagg, for the MINOS Collaboration
Tufts University, 4 Colby Street, Medford, MA, USA 02155

As of December 2005, the MINOS long-baseline neutrino oscillation experiment collected data with an exposure of 0.93×10^{20} protons on target. Preliminary analysis of these data reveals a result inconsistent with a no-oscillation hypothesis at level of 5.8 sigma. The data are consistent with neutrino oscillations reported by Super-Kamiokande and K2K, with best fit parameters of $\Delta m_{23}^2 = 3.05^{+0.60}_{-0.55} \times 10^{-3}$ and $\sin^2 2\theta_{23} = 0.88^{+0.12}_{-0.15}$.

1. Introduction

The MINOS long-baseline neutrino oscillation experiment [1] was designed to accurately measure neutrino oscillation parameters by looking for ν_μ disappearance. MINOS will improve the measurements of $\Delta m^2 23$ first performed by the Super-Kamiokande [2, 3] and K2K experiments [4]. In addition, MINOS is capable of searching for sub-dominant $\nu_\mu \to \nu_e$ oscillations, can look for CPT-violating modes by comparing ν_μ to $\bar{\nu}_\mu$ oscillations, and is used to observe atmospheric neutrinos [5].

The MINOS experiment uses a beam of ν_μ created at Fermilab National Laboratory and directed at the Soudan mine in northern Minnesota, a distance of 735 km. The composition and energy spectrum of the beam is measured in two detectors, the Near (1 km downstream from the target) and the Far (735 km downstream), allowing for precision measurements of the spectral distortion of the beam.

2. The NuMI Neutrino Beam

The Fermilab Main Injector has a minimum cycle time of 1.87 s, with a maximum intensity of 4×10^{13} protons per pulse for a maximum average power of 0.4 MW of power on the target. Protons are extracted from the Main Injector in a single turn, taking $\sim 10\mu$s.

The NuMI neutrino beam [6] is created by directing these protons onto a water-cooled segmented graphite target. Secondary pions from the proton-carbon interactions are deflected into the forward direction by two parabolic focusing elements (horns) before being allowed to decay in a 675 m evacuated decay volume. Undecayed secondaries are stopped by an absorber wall at the end of this volume. The primary proton beam is monitored for position and intensity on target. The secondary hadrons and muons are monitored for position and intensity to ensure good alignment and composition of the beam.

The NuMI beam has been in operation since late 2004. Near the end of 2005, a total exposure of 0.93×10^{20} protons were delivered to the target. This exposure was used in the following analysis. At the end of the run period in March 2006, the maximum intensity delivered to the target was in excess of 25×10^{12} protons per pulse, with a maximum target power of 250 kW.

3. The MINOS Detectors

The MINOS Near and Far detectors are constructed to have nearly identical composition and cross-section. The detectors consist of sandwiches of 2.54 cm thick steel and 1 cm thick plastic scintillator, hung vertically. The polyethylene scintillator is in the form of 4 cm-wide strips, with a co-extruded TiO_2 reflective coating. Along one side of each strip a groove holds a glued wavelength-shifting optical fibre. Scintillation light created in the scintillator is caught by the fibre, shifted, and transported efficiently to the end of the strip. Clear readout fibres carry the light to multi-anode photomultipliers for readout.

The detectors act as tracking, sampling calorimeters. Strips in adjacent planes are oriented orthogonally, allowing events to be reconstructed in two transverse views. Both detectors are equipped with magnet coils which generate $\sim$1.2 T toroidal magnetic fields, which act to contain long muon tracks and provide curvature information for estimating energies.

The Near detector has a total mass of one kiloton, and 282 of these steel planes, 153 of which are instrumented. It uses sampling electronics to distinguish neutrino events in time, due to the large instantaneous intensity during a beam spill. The Far detector masses 5.4 kilotons, and consists of 485 steel planes, 484 of which are instrumented. Because of the low rate in the Far detector, the strips are read out via an 8-fold optical multiplexing.

4. Data Selection

Charged-current ν_μ events in the MINOS detectors appear as long muon tracks accompanied by short hadronic showers near the event vertex. The two other distinguishable event classes are neutral-current events, which appear only as short, sparse hadronic showers, and ν_e charged-current events, which appear

as short, dense electromagnetic showers. For this analysis, only charged-current ν_μ events are considered.

Neutrino events are selected by first taking time-coincidence with the beam spill. This is performed by hardware trigger in the Near detector. In the Far detector candidate events are required to occur at $2449 \pm 50\mu s$ after beam spill (the time-of-flight for neutrinos traveling to Soudan). Charged-current ν_μ events require a well-reconstructed track in both scintillator views, and confinement of the track vertex to the defined fiducial volumes of each detector. The curvature of the track is selected to be consistent with a μ^-. Finally, charged-current ν_μ events must pass a particle identification cut, which relies on event length, the proportion of calorimetric energy in the shower, and the track dE/dx. These variables are assembled into a probability density functions and used to create a likelihood-based particle ID parameter shown in Figure 1. A cut is performed on this variable to select a pure ν_μ CC sample. The total efficiency and purity of this selection is shown in Figure 2.

Figure 2: Purity and Efficiency of the CC ν_μ Event Selection. Efficiency and purity are shown as a function of reconstructed event energy, using Monte Carlo. Contamination events are from NC events, almost entirely at low reconstructed energy.
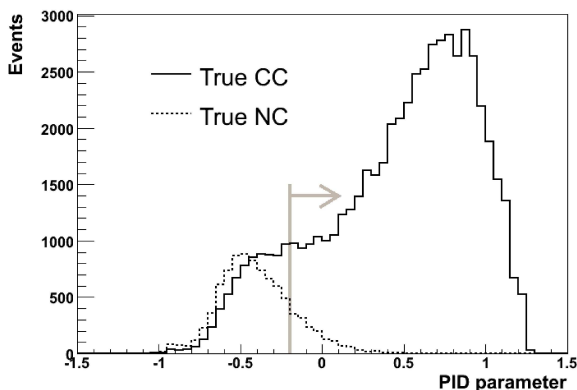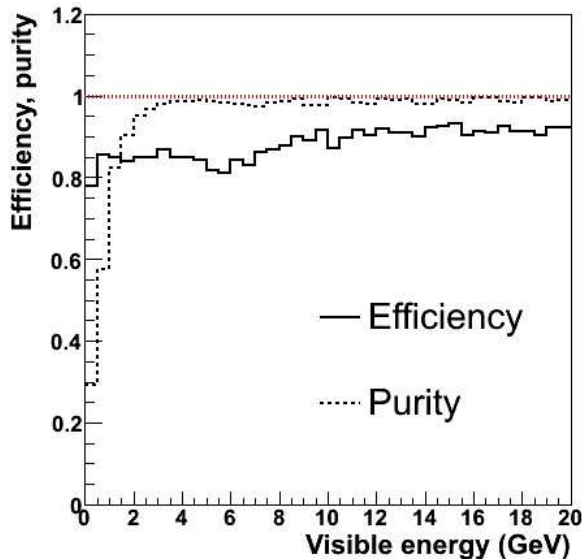

Figure 1: The Particle ID Cut. The solid line shows the distribution of Monte Carlo charged-current events and the dashed line shows the distribution of Monte Carlo neutral-current events as a function of the particle ID parameter used for the selection. The cut value is shown.

For selected events, the neutrino energy is reconstructed by taking the sum of the muon energy and the shower energy. Muon energy is found using the range of the muon (if contained) with an accuracy of 6%, or by using the muon curvature (if uncontained) with an accuracy of 10%. The shower energy is found using calorimetry, with an uncertainty of approximately $55\%/\sqrt{E}$.

5. The Near Detector Spectrum

The Near detector neutrino sample is used as the control in the experiment, providing the unoscillated beam spectrum. One of the advantages of the NuMI

beam is that the target may be moved relative to the horns, allowing a varying focus of the pions and therefore different neutrino energies. Three such settings are used to create 'high', 'medium' and 'low' energy beams. Although the bulk of data was taken in the low energy configuration (to maximize sensitivity at the oscillation minimum) data was also taken in the other configurations to test beam modeling in the Near detector.

Monte Carlo simulation of the beam predicted the neutrino flux for all beam configurations to within 10%. The residual disagreement was a strong function of beam configuration rather than neutrino energy, implying that the simulation error was due to the modeling of the secondary pions. An empirical function was used to modify the secondary pion simulation as a function of x_f and p_t. This function was fit to data from all configurations. These data and their associated Monte Carlo spectra are shown in Figure 3.

The measured Near detector spectrum was used to predict the Far detector spectrum. First, the observed Near detector reconstructed energy spectrum was corrected for purity and efficiency to obtain the true neutrino spectrum.

Second, the spectrum was corrected for the difference in solid angles subtended by the Near and Far detectors. The smaller range of angles observed by the Far detector results in a narrower spectrum relative to the Near detector. This difference can be robustly estimated by using knowledge of the pion two-body decay kinematics and the geometry of the NuMI
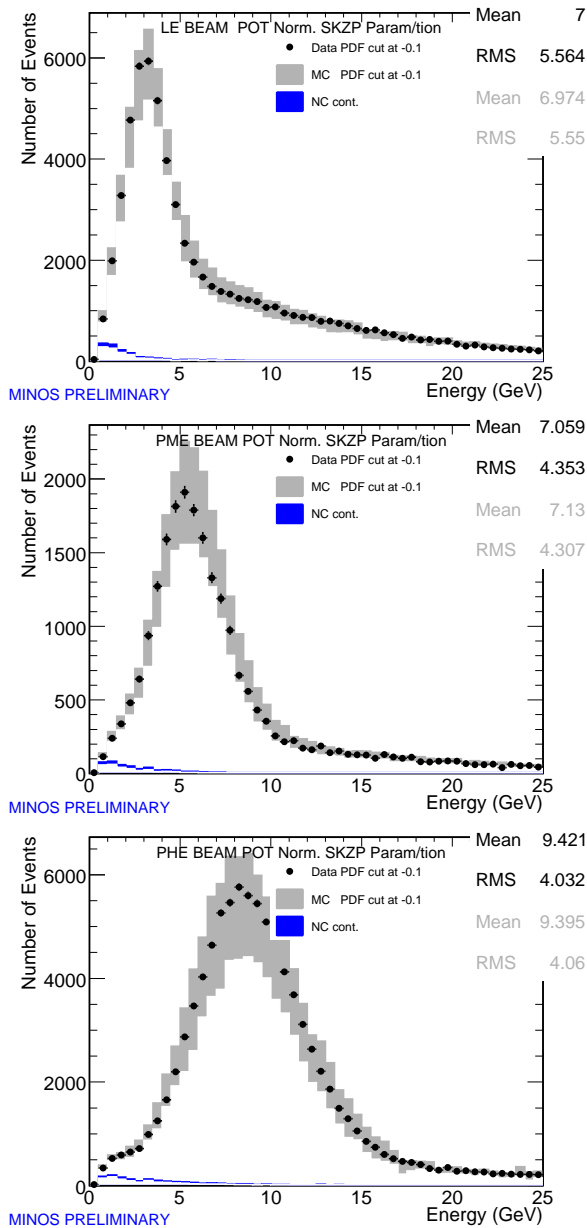
Figure 3: Near Detector Neutrino Energy Spectra. The spectrum of observed charged current dots. Hatched areas indicate the Monte Carlo prediction of the spectrum, after tuning. The predicted neutral current contamination is shown in blue. The top plot shows the data from the low energy beam configuration, the middle plot shows the medium energy configuration, and the lower plot shows the high energy configuration.

beamline. Using the beam Monte Carlo, a matrix is created that transforms a true Near detector spectrum into a true Far detector spectrum.

Last, the predicted true Far detector spectrum is simulated by Monte Carlo to create an expected reconstructed neutrino spectrum which can be compared to data.

6. Far Detector Results

The observed reconstructed neutrino spectrum at the Far detector is shown in Figure 4. The data do not agree with the unoscillated prediction; this null hypothesis is excluded at 5.8 sigma. When fitted to a two-neutrino oscillation hypothesis, a fit is found with reasonable probability within a parameter space shown in Figure 5. In this fitting procedure, only statistical errors were considered.

Systematic errors were estimated by taking Monte Carlo data samples simulated near the best fit point for the data. Systematic errors were introduced to the Monte Carlo and not corrected in analysis. The resulting shift in the best fit point is taken as the systematic error on that parameter. The systematic errors considered are shown in Table I. These systematics are briefly discussed below.

Normalization changes the overall expected number of events at the Far detector, based upon a combination of uncertainty on protons-on-target and the fiducial mass. This is known to 4%.

Muon energy scale is the uncertainty on the average energy of muons due to incorrect steel density or magnetic field modeling. This is known to 2%.

Relative shower energy scale is the degree of confidence to which the hadronic calorimetry in the Near detector matches that in Far. The energy scale between these two detectors after calibration should agree to within 3%.

NC contamination is the uncertainty on the number of neutral current background events erroneously accepted into the charged current sample. A conservative error of 30% is used.

CC Cross section is allowed to vary in several ways: the KNO parameters governing the relative fraction of resonance to deep inelastic scattering fraction were allowed to change by 20%, and the axial mass for quasi-elastic events and resonance events were allowed to change by 5%.

Beam uncertainty is the difference in measured parameters given that the data is fit without retuning the Monte Carlo beam simulation to the Near detector data. That is, an incorrect beam matrix was used to extrapolate the beam to find the shift in fit values.

Intra-nuclear rescattering gives the uncertainty due to poor modeling of the energy loss of pions scattered or re-absorbed as they leave the target nucleus. This energy cannot be detected, and so an uncertainty on this interaction creates an uncertainty on the absolute hadronic shower energy scale at both detectors.

Description	$\Delta\left(\Delta m_{23}^2\right)$	$\Delta\left(\sin^2 2\theta_{23}\right)$
Normalization $\pm$ 4%	0.63×10^{-4}	0.025
Muon energy scale $\pm$ 2%	0.14×10^{-4}	0.020
Relative Shower energy scale $\pm3\%$	0.27×10^{-4}	0.020
NC contamination $\pm$ 30%	0.77×10^{-4}	0.035
CC cross-section uncertainties	0.50×10^{-4}	0.016
Beam uncertainty	0.13×10^{-4}	0.012
Intra-nuclear re-scattering	0.27×10^{-4}	0.030
Total Systematic Error	1.19×10^{-4}	0.063
Total Statistical Error	6.4×10^{-4}	0.15

Table I *MINOS PRELIMINARY* Systematic Uncertainties. Systematic effect on the data are shown together with the shift incurred by not correcting for these systematics on the best-fit point of Δm_{23}^2 and $\sin^2 2\theta_{23}$.

Table I also shows the sum of these systematic errors taken in quadrature, as compared to the statistical errors. It can be seen that for this limited data set, MINOS is statistically limited. Systematic errors have a negligible effect on the contour at this sensitivity.
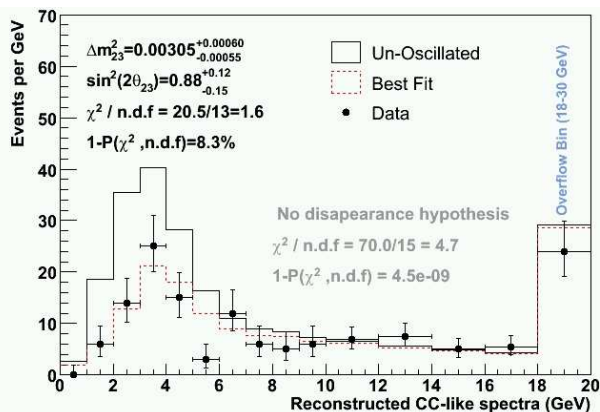

Figure 4: *MINOS PRELIMINARY* Far Detector Energy Spectrum. The predicted spectrum in absence of oscillations is shown by the solid curve. The dashed curve represents a fit to the data by an oscillation hypothesis with a best fit of $\Delta m_{23}^2 = 3.05^{+0.60}_{-0.55} \times 10^{-}3$ and $\sin^2 2\theta_{23} = 0.88^{+0.12}_{-0.15}$

.

7. Conclusions

MINOS has completed a preliminary analysis of the first $\sim 10^{20}$ protons on target, and found a result incompatible with no oscillations at a significance level of 5.8 sigma. The signal is consistent with oscillations seen by Super-Kamiokande and K2K at the 90% confidence limit. Systematic errors are believed to be under control at the limit of the current statistics. This result will significantly improve the world average on $\Delta m_2^2 3$.
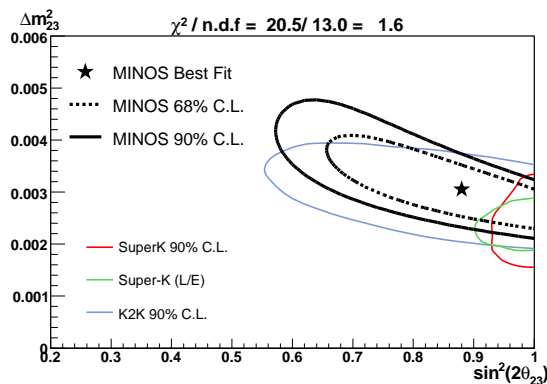

Figure 5: *MINOS PRELIMINARY* Allowed Region. The black solid (dashed) line shows the MINOS 90% (68%) confidence limit in Δm_{23}^2 and $\sin^2 2\theta_{23}$. The 90% confidence regions from the Super-K zenith-angle analysis [2], the Super-K L/E analysis [3] and the K2K result [4] are shown in red, green, and blue respectively. The contour is described by statistical errors only.

MINOS currently has a data sample of approximately 1.5×10^{20} protons on target, and will be analyzing this expanded data set for summer 2006. MINOS intends to continue collecting data until at least 2010, at which time it's physics sensitivity is expected to be considerably improved.

Acknowledgments

References

[1] M. A. Thomson, Nucl. Phys. Proc. Suppl. **143**, 249 (2005).

[2] Y. Fukuda *et al.* [Super-Kamiokande Collaboration], Phys. Rev. Lett. **82**, 2644 (1999) [arXiv:hep-ex/9812014].

[3] Y. Ashie *et al.* [Super-Kamiokande Collaboration], Phys. Rev. D **71**, 112005 (2005) [arXiv:hep-ex/0501064].

[4] E. Aliu *et al.* [K2K Collaboration], Phys. Rev. Lett. **94**, 081802 (2005) [arXiv:hep-ex/0411038].

[5] P. Adamson *et al.* [MINOS Collaboration], Phys. Rev. D **73**, 072002 (2006) [arXiv:hep-ex/0512036].

[6] S. E. Kopp, arXiv:physics/0508001.